FLUID DYNAMIC DESIGN AND ANALYSIS OF A HIGHLY LOADED CENTRIFUGAL ROTOR FOR MINI ORC POWER SYSTEMS

Salvatore Vitale[1*], Matteo Pini[1], Antonio Ghidoni[2] and Piero Colonna[1]

[1] Delft University of Technology, Propulsion and Power,
Delft, The Netherlands
s.vitale@tudelft.nl

[2] Universita' degli studi di Brescia, Department of Mechanical and Industrial Engineering,
Brescia, Italy

* Corresponding Author

ABSTRACT

This article presents the fluid-dynamic design and analysis of a high-loaded centrifugal rotor for mini ORC applications. Recently a vast interest about mini ORC turbogenerators is growing up. These systems must be equipped with high-efficient turbines to maximize their overall efficiency. Recent works demonstrated that, among the various alternatives, the multi-stage centrifugal turbine may be extremely attractive for such applications. However, this turbine is characterized by a very high loaded first stage whose design has a key role for the success of the technology. In order to cope with these severe conditions we propose a design methodology specifically tailored for radial-outflow cascades. The method combines NURBS curves and flow passage area control to "physically" drive the construction of the profiles. As exemplary test case, we apply the new procedure to the design of the first rotor of a $10kW_e$ micro centrifugal turbine for heat recovery application. Finally, we assess the performance of the designed rotor by means of 2D and 3D turbulent simulations, providing an extensive comparison against preliminary estimates based on Traupel and Craig&Cox loss correlations. The results show that the design method is flexible and quick enough to minimize losses by few manual iterations. Furthermore, it turned out that both loss models fairly well estimate profile losses, even if Traupel seems to be more accurate than Craig&Cox model to predict secondary and tip clearance loss effects.

1. INTRODUCTION

Organic Rankine Cycles (ORC) power systems are, nowadays, a well-established technology for the conversion of thermal energy sources in the small-to-medium power range (from 100 kWe to few MWe), D'Amelio (1935); Tabor and Bronicki (1964); Angelino et al. (1984); Verneau (1987). Miniaturized (5-30 kWe) systems are particularly attractive for waste heat recovery onboard mobile applications, e.g. trucks or aircrafts, and for decentralized energy production in combination with solar heat sinks.

The realization of successful mini ORC (*m*ORC) power systems demands to desigh highly efficient (>75%) mini-turboexpanders, to be competitive with respect to existing alternatives like fuel-cells. As well documented, the use of organic media generally leads to unusual turbine configurations, Macchi (1985, 1977): few axial stages or a single centripetal stage, often characterized by supersonic flows and strong shocks. These phenomena are even worse in small blade passages, due to the interaction with tip and secondary vortex structures. The achievement of high-efficient mini-turbines implies a full redefinition of the design strategy of the expander, starting from the turbine concept, passing through dedicated preliminary design optimization, Pini et al. (2013); Casati et al. (2014), and eventually arriving at a complete new definition of the optimal blade profiles through advanced methodologies, Persico et al. (2013); Pini et al. (2014).

Recently, the multi-stage radial-outflow turbine (ROT) has been thoroughly studied for ORC power sys-

tems. This configuration naturally accommodates the high volumetric flow ratios typical of ORC fluids and allows for compact multi-stage arrangements, thus preventing high supersonic flows. Although in a previous work the authors already demonstrated with a preliminary investigation that ROT may allow for compact and efficient turbo-expanders for *m*ORCsystems, Casati et al. (2014), many challenges are still to be addressed for the success of this architecture. One of the open issue regards the design and performance evaluation of the first stage, which operates under very unfavorable flow conditions. Notably, this stage usually features a rotor characterized by high flow deflection, low aspect ratio and significant tip-to-blade height clearance, resulting in low fluid dynamic performance that may compromise the efficiency of the whole machine. Moreover, the rotor is subject to non-inertial effects, i.e. centrifugal and Coriolis fictitious forces, and to a high increase of the flow passage in the radial direction that pose additional concerns during the blade design process.

Consequently, demonstrating that the first rotor can be designed with acceptable efficiency is crucial to quantify the actual gain offered by the ROT concept for *m*ORCwith respect to axial and radial-inflow competitors. For this reason the objective of this work is to perform a trustworthy fluid dynamic design of the first rotor of a 5-stages small centrifugal turbine preliminary which was designed following the methodology provided in Casati et al. (2014). The study is supported by detailed 2D and 3D CFD analysis and complemented by a comparison between the computed and predicted (by means of the widely used empirical correlations Craig and Cox (1971); Traupel (1977)) loss coefficients.

The blade profile definition is carried out by a novel methodology for the aerodynamic design of centrifugal blades based on NURBS curves and flow passage area detection. The algorithm is implemented in a new CAD Turbine Blade Modeler (TBM) exploiting the Python API of the open-source (LGPL License) Software FreeCAD Falck and Collette (2012). The TBM is in turn automatically linked with two in house mesh generators (named UMG2 and UMG3, respectively) to create high quality 2D and 3D grids. The flow calculations are carried out by resorting to the SU2 solver, recently extended by the authors to deal with arbitrary thermo-physical models Vitale et al. (2015).

The paper is organized as follows: Section 2 illustrates the procedure devised for the design of centrifugal cascades, Section 3 extensively describes the design of the first rotor of a *m*ORC for heat recovery applications, while section 4 analyses the performance of the considered cascade with blade-to-blade and 3D simulations.

2. METHODOLOGY

This section briefly recalls the tools adopted in this work and reports extensively the methodology devised for the design of centrifugal blades.

2.1 Numerical Methods

The CFD solution is obtained by coupling the in-house mesh generation software UMG2 and UMG3, Ghidoni et al. (2006), to the SU2 suite. SU2 discretizes and solves the fluid governing equations using the finite volume approach on unstructured grids. The code has been recently extended by the authors to treat non-ideal compressible fluid flows that commonly occur in ORC turbines. An exhaustive description of the solver characteristics alongside the numerical validation process can be found in Vitale et al. (2015).

2.2 Centrifugal Blade Construction

In the centrifugal architecture the peripheral speed does not change along the blade span allowing to resort to untwisted blades. For this reason, the construction of a centrifugal blade reduces to the definition of a 2D blade profile simply lofted to construct the 3D geometry.

Figure 1 illustrates the construction of the centrifugal camber-line using NURBS curve. The camber-line is completely defined by the inlet blade angle β_{in}, the outlet blade angle β_{out}, the stagger angle γ, the radial chord c_{rad} and the *LE* position. As a matter of fact the *TE* position is uniquely defined by the *LE*,

γ and c_{rad}, and an additional third point P_{int} resulting from the intersection of the inlet and and outlet lines. These two lines follow the direction of β_{in} and β_{out}, respectively, which are defined in the radial reference of framework.

Using three *CPs* the camber-line assumes a quadratic shape, and changing the weight value of the intersecting control points the ensemble of the quadratic curves can be represented as an arc of parabola (w_{int} = 1.0), hyperbole (w_{int} > 1.0), ellipse or circle (w_{int} < 1.0) Piegl and Tiller (1997).

The approach used for the construction of the pressure and suction side is based partially on the work of Vestraete (2010) for the construction of 2D axial turbine blade. The *SS* and *PS* are NURBS curves themselves whose shape is specified by distributing the *CPs* according to a thickness law as a function of the camber-line length. Figure 2 shows an example of *TD* for the suction side, and, on top, the corresponding distribution of the *CPs* on the *SS* along the blade camber-line. It is worth to note that by properly tuning the *TD* law any desired blade loading trend can be met.

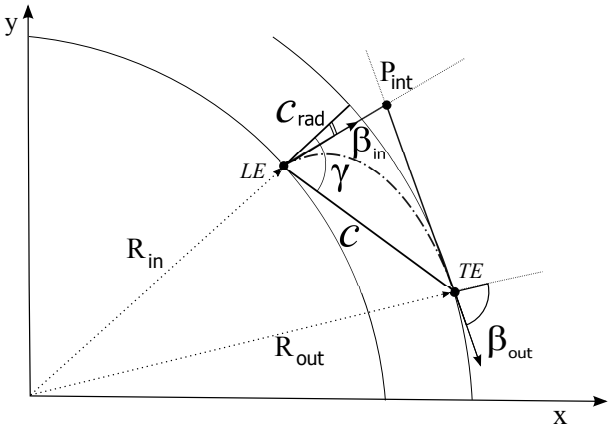

Figure 1: Camber-line construction for a centrifugal turbine using NURBS curve.

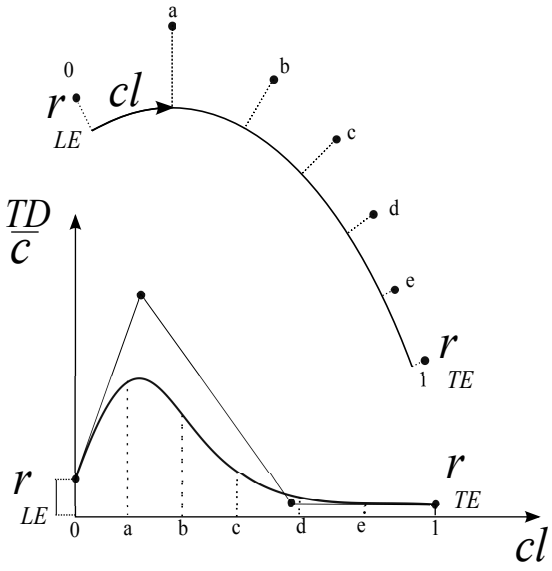

Figure 2: 2D centrifugal profile construction using NURBS curve.

3. 2D DESIGN OF A CENTRIFUGAL ROTOR FOR MINI-ORC APPLICATIONS

This section presents the design of a high loaded centrifugal rotor by using the TBM and the NICFD solver in an iterative manner to attain a convenient blade shape.

3.1 Design of the Rotor Blade

We here consider the first rotor of the 5-stage small-scale transonic ROT as exemplary test case. The total-total efficiency of the machine was predicted by the Traupel's loss model to be approximately 80%. The main data for the blade geometry construction and the boundary conditions for the CFD simulation are provided in Table 1 and 2, respectively. Figure 3 shows the trends of the main parameters influencing the performance of the turbine cascades: blade deflection, aspect ratio and the tip clearance. The first rotor (blade row n°2 in Fig.3) is characterized by the most severe conditions: extremely high flow deflection, low aspect ratio and high tip clearance to blade height ratio. Additionally, Fig. 4 reports the relative increase of the passage area and peripheral speed of each blade row for the same turbine. Due to the high increase of the peripheral speed along the stream-wise direction, the first rotor is furthermore subject to a significant rise of the (relative) fluid mechanical energy from the inlet to the outlet. As a consequence, higher Mach numbers are expected to occur at the rotor outlet compared to stationary cascades of similar geometry, working under the equivalent expansion ratio. On the other hand, if not properly handled, the radial evolution of the machine may lead to unexpected converging-diverging passage areas even

adopting purely converging blades with sudden flow supersonic excursions and generation of strong shocks.

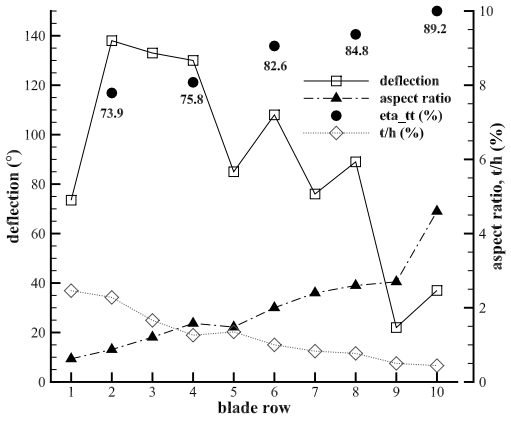

Figure 3: Flow deflection, aspect ratio, tip clearance for each blade row and total total efficiency for each stage of the 5-stage mini centrifugal turbine.

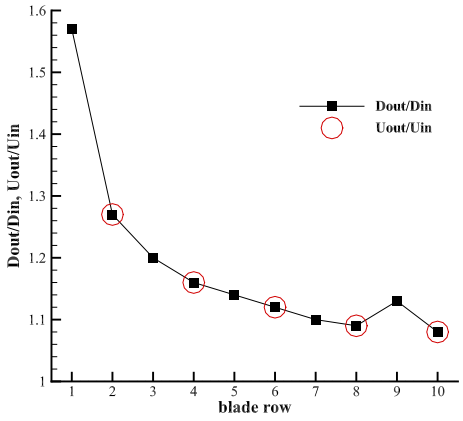

Figure 4: Rate of increase of the diameter for each blade row and of the peripheral speed for each rotor blade of the 5-stage mini centrifugal turbine.

The design of centrifugal profiles cannot follow any standard design rule established for axial cascades, as already pointed out in Persico et al. (2015), where the analysis was restricted to slender profiles for low deflection radial cascades and suggested rather simple design criteria, i.e. elliptic mean-arc and thickness distribution taken from existing profiles, that are almost useless in presence of high-loaded blades with relevant radial area evolution. Hence, we adopt the more general approach explained in the previous section to achieve a suitable blade profile for such unconventional configuration.
As anticipated the degrees of freedom for the 2D profile are the stagger angle γ and the thickness distribution for the pressure (TD_{PS}) and suction side (TD_{SS}). R_{in}, c_{rad}, β_{out}, N°_{blades}, TE_{th} are the inputs for the TBM, while the prescribed blade throat width o_{out} is achieved by selecting the appropriate TD_{PS}, TD_{SS}, and γ.

R_{in}	1.88 cm
c_{rad}	0.5 cm
β_{in}	66.0 °
β_{out}	-74.1 °
N°_{blades}	38 [-]
o_{out}	0.1 cm
te_{th}	100 μm

Table 1: Geometrical parameters for the desing of the rotor blade.

Fluid	D4
$T_{t,in}$	305.79 °*C*
$P_{t,in}$	3.66 *bar*
$P_{s,out}$	1.655 *bar*
$\beta_{flow,in}$	66.0 °
N	19000.0 rpm

Table 2: Main input data for the CFD simulation.

Figure 5 shows the designed rotor cascade. As highlighted in the top picture of Fig. 6, the radial evolution of the cascade dictates an unusual non-monotonic trend of the flow passage area (PA). The inlet semi-bladed region is characterized by a throat located where the flow encounters the *SS* at the *LE*. Then the PA increases until the flow reaches the *PS*. If not conveniently controlled this trend may generate undesired supersonic flow bubbles with high risk of flow separation on the *SS*. Consequently strong adverse pressure gradients may establish on both pressure and suction sides with the increasing of the boundary layer. Also in the semi-bladed outlet region the PA increases, triggering the onset of strong shock waves on the suction side.

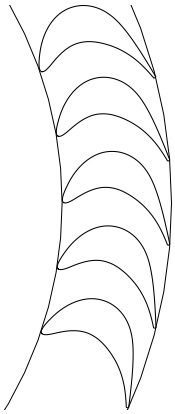

Figure 5: Centrifugal rotor 2D profile.

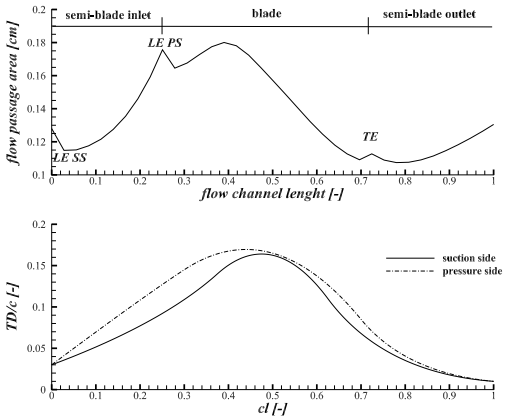

Figure 6: Flow passage area distribution and TD_{SS} and TD_{PS} of the 2D centrifugal rotor.

The optimal rotor configuration should mitigate all these loss mechanisms. The final blade shape was derived by iteratively changing the TD_{SS}, the TD_{PS} and the γ. Each blade profile was tested by means of 2D viscous simulations using the SST turbulence model and few design adaptations were necessary to minimize the fluid-dynamic losses. The bottom picture of Fig. 6 displays the final TD_{SS} and TD_{PS} laws used to construct the final profile. A value of 22.5 was set for the stagger angle. It can be observed that the *LE* thickness is thin, especially on the *SS*, in order to avoid the creation of a throat in the semi-bladed inlet region; in the middle part the profile is rather thick so as to better guide the flow and prevent separations; the *TE* is conversely set to the smallest value, compatible with manufacturing limits, in order to reduce wake and mixing losses. Figure 7 shows the relative Mach contour of the designed centrifugal rotor; it can be appreciated that no shocks appear upstream of the blade and no flow separations occur on both suction and pressure sides. As expected, shock waves are clearly visible downstream of the blade as a result of the flow over-expansion on the rear suction side.
A further improvement of the rotor performance can be certainly achieved by means of shape optimization algorithms. However, as demonstrated, a thorough understanding of the physical problem can already aid the initial design of the cascade without the need of expensive optimization procedures. Furthermore, the present algorithm can greatly help to drive the automated design algorithms in the early steps.

4. NUMERICAL VERIFICATION OF THE CENTRIFUGAL ROTOR

In this section we illustrate the fluid-dynamic performance of the designed high loaded centrifugal rotor by means of blade-to-blade and fully 3D simulations.

4.1 2D CFD analysis

The blade-to-blade performance of the final rotor configuration are now discussed in detail. The siloxane D4 is modeled as a polytropic Peng-Robinson gas. Table 3 summarizes the main results of the 2D simulation. The profile losses are estimated by resorting to the mixed-out average at inlet section and at a section placed 5% of the radial chord downstream of the trailing-edge. At nominal conditions the corresponding kinetic energy loss coefficient is nearly 3.9%, while values predicted by the Traupel's and Cox's model are about 3.2% and 5%, respectively. Considering that these correlations were developed for axial cascades, we can conclude that, at least at a preliminary level, they provide a reasonable measure of the 2D performance of the cascade and can be used in the design phase of *m*ORC.

$\dot{m}_l$	1.64 $kg/s/m$
M_{out}	1.05 [-]
$\beta_{out,flow}$	74.49 °
ζ_{is}	3.9 [-]

Table 3: Main results of the blade to blade simulations

When assembling the full row we considered the number of blades as a fixed input from the preliminary design phase. However, as well known in turbomachinery theory, the solidity largely affects the overall fluid-dynamic performance of the cascade. In case of radial *m*ORCthe direct application of the solidity correlations for axial turbines is somewhat questionable and therefore accurate numerical predictions may be necessary to determine the optimal value. Figure 8 presents a study of the optimal number of blades to minimize the profile losses. All the profiles have the same TD_{SS} and TD_{PS}, yet a different stagger angle in order to keep constant the gauging angle $\left(\frac{o}{s}\right)$. The minimum profile losses arises for 38 blades, surprisingly in accordance with the number of blades estimated by the Zweifel criterion, Zweifel (1945), and used in the preliminary design phase. Figure 9 shows that in all cases two successive shock waves occur on the suction side though of different intensity. The first shock, that is weaker for the row with 32 blades, is generated by the interaction of the suction flow with the expansion fan impinging on the suction side. It is interesting to note that increasing the number of blades the flow experiences larger acceleration on the suction side, leading to a stronger fishtail shock wave. All these phenomena are amplified by the diverging shape of the streamtube along the radial direction, which emphasizes the flow accelerations and arrests. An opposite trend manifests just upstream of the trailing-edge. The reduction of blade loading induces lower velocities and adverse pressure gradients, resulting in a much weaker second shock for the case with 45 blades. The profile losses are greatly influenced by the combination of these two shocks and the final optimum solidity is reached with 38 blades, which may represent the trade-off between the two opposite situations.

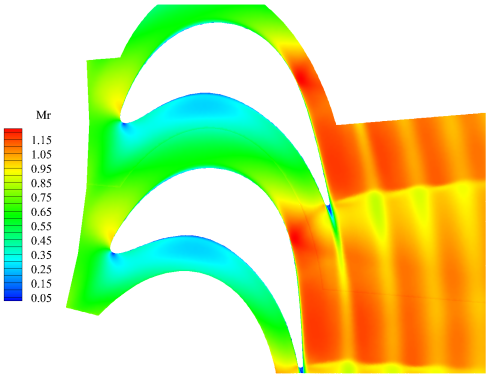

Figure 7: Mach contour of the designed centrifugal rotor.

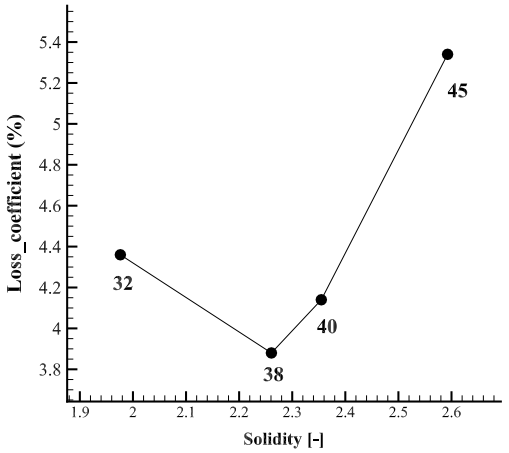

Figure 8: CFD blade to blade results of the solidity optimization for the centrifugal rotor.

Besides the major role on the fluid dynamic losses, the solidity parameter influences the flow slip and, eventually, the work extraction from the radial cascade. Figure 10 shows the angular difference between the rotor simulated as a rotating cascade and as a stationary cascade (provided consistent relative boundary conditions) for different number of blades. In order to avoid any post expansion and post compression effect, that can modify the outlet flow angle, the boundary conditions for the static case are chosen to obtain the same averaged flow Mach number at the outlet. The results are qualitatively in

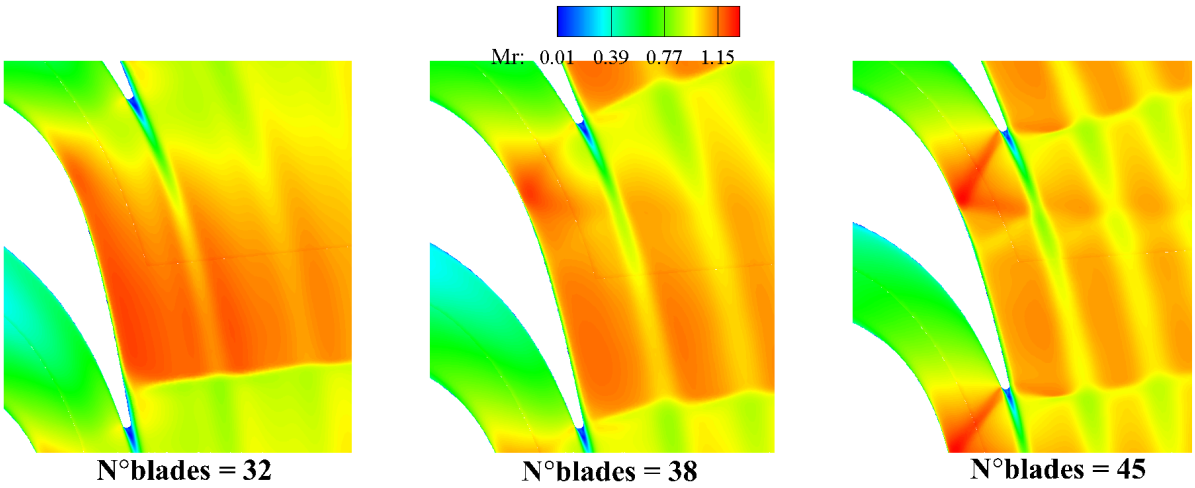

Figure 9: Rotor profile and its blade channel curve.

agreement with the general theory of circulation, which admits, for purely radial cascades, the presence of a counter-rotating vortex acting on the blade to blade plane ($\nabla W = -2\omega$). The net effect is the appearance of a fictitious force deflecting the flow (slip effect) in the tangential direction, namely in the opposite direction to the verse of rotation of the turbine. As expected, the slip vanishes for a high number of blades, as occurs in the first rotor of *m*ORCturbines.

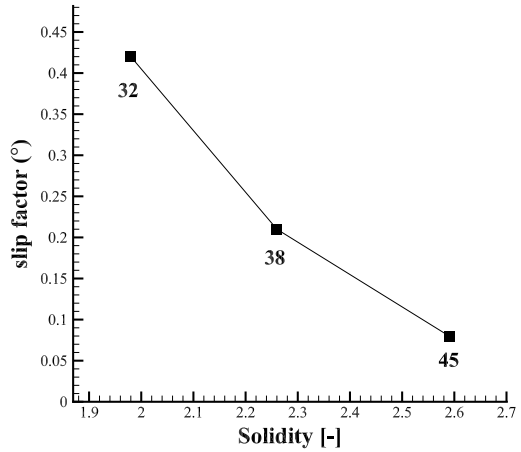

Figure 10: Slip factor for 3 centrifugal cascade with 32, 38 and 45 blades.

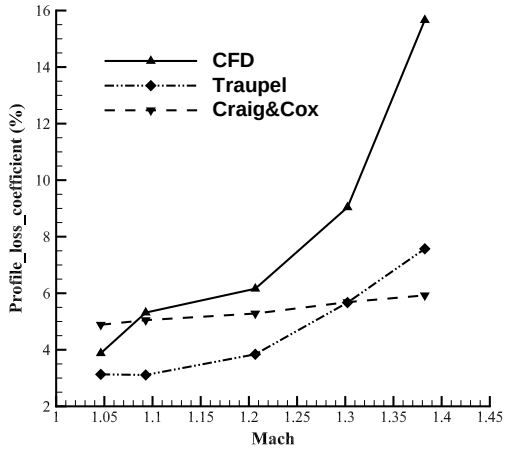

Figure 11: Comparison of the profile losses estimation.

Another key aspect of the radial cascades is their behaviour at off-design conditions. This is particularly relevant for small-scale turbines, as their functioning is intimately connected to the energy demand of the load. The blade to blade analysis of the 38 blade cascade is herein extended at moderate partial loads, until reaching an outlet Mach number of 1.4. To aid the reader we remember that Mach 1.4 is the traditional design limit in axial configurations to retain purely converging blades. The objective of the study is twofold: to assess the reliability of the correlations, and to gain knowledge about the characteristic of converging centrifugal blades for weakly supersonic flows. The outcomes are illustrated in Fig.11. As well visible, the results show that up to Mach 1.2 the predictions of the loss models are fairly in accordance with CFD results. While the C& C correlation displays a smaller deviation and fails to capture the correct slope of the loss curve, the Traupel's correlation provides a more reliable trend, even if it underestimates the losses for the whole range of operating conditions. This suggests that using such

correlations for weakly and fully supersonic flows in *m*ORCturbines may result in the over-prediction of the expander total-to-total efficiency. Likewise some general recommendations can be drawn on the basis of the CFD predictions. The exponential-like growth of the rotor losses above Mach 1.2 indicates that radial-outward converging blades optimized for transonic regimes may suffer of severe drawbacks already at moderate off-design conditions, strengthening the idea that robust fluid-dynamic design of mini-ROT can be truly achieved by fully multi-stage robust optimization procedures.

4.2 3D CFD analysis

This section briefly describes the 3D CFD analysis of the rotor cascade. As previously mentioned the 3D profile is generated simply lofting the 2D profile. The blade height (*blh*= 0.43 cm) is calculated by using the linear mass flow computed with the blade to blade analysis and the expected mass flow ($\dot{m}$ = 0.266 kg/s) of the turbine ($blh = \frac{\dot{m}}{\dot{m}_l}$).

Three 3D configurations have been considered to investigate the different loss mechanisms occurring in the 3D blade passage: a geometry i) with slip end-walls to determine the profile losses, ii) with no slip end-walls to estimate secondary flows, and iii) with a tip clearance *tcl* = 100μm and *tcl* = 200μm to examine the tip loss mechanism.

The calculations were performed using the same boundary conditions specified for the 2D case and unstructured meshes of about 3 million elements. Convergence was approximately reached after 10000 iterations (10 hours on 20 cores, Intel®Xeon(R) CPU E5-2687W 3.10GHz).

Table 4 shows the breakdown of the loss sources. As expected the tip clearance losses highly penalize the performance of small-scale ORC cascades. As a matter of fact, as depicted in Fig. 13, even with *tcl* over *blh* around $\frac{1}{40}$, the tip clearance vortex covers about 25 % of the flow passage area. Such vortex structure causes a considerable distortion of the flow angle at tip, see Fig. 12, which eventually leads to a lower averaged outlet flow angle and, hence, a significant reduction of work extraction. Indeed a even worse situation would occur by doubling the *tcl* to 200 μm. Finally, Table 5 compares the fluid dynamics losses estimated by the CFD and empirical correlations. The C & C model fails in predicting the secondary and tip losses whereas the Traupel, though with some overestimation, better captures the trends.

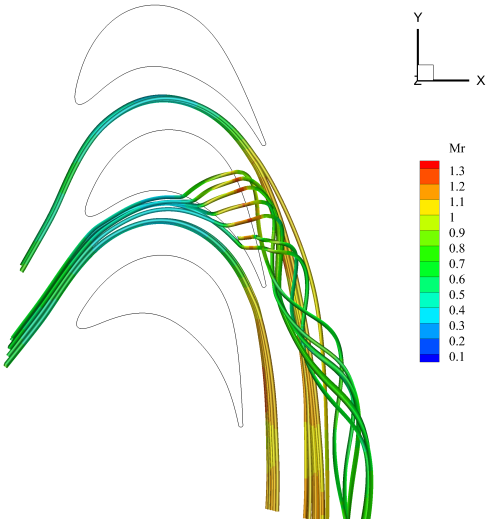

Figure 12: 3D stream lines of the flow solution with tip clearance 100 μm top view.

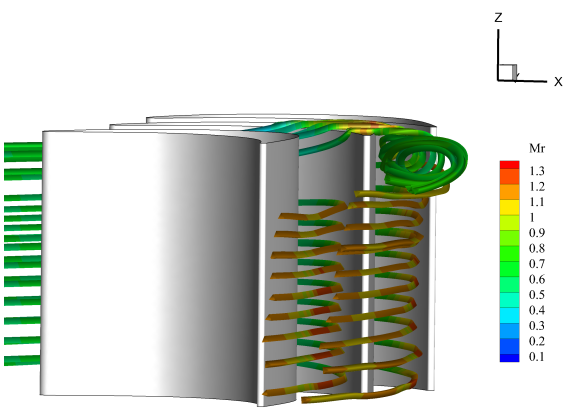

Figure 13: 3D stream lines of the flow solution with tip clearance 100 μm downstream view.

5. CONCLUSIONS

This work illustrated the application of a novel blade design methodology to the development of a high loaded centrifugal blade for mini-ORC turbines. The use of a physical-based approach allows to obtain a

case	$\zeta_{is,tot}$	$\beta_{flow,out}$	ew
Blade to blade	3.9	74.5	6.84
3D no tip	7.3	74.4	6.66
3D 100 μm tip	17.0	72.24	6.20
3D 200 μm tip	24.8	70.5	6.05

Table 4: Main results of the simulations.

tool	$\zeta_{is,p}$	$\zeta_{is,s}$	$\zeta_{is,tcl,100}$	$\zeta_{is,tcl,200}$
CFD	3.9	3.4	9.7	17.5
C & C	4.9	11.7	3.8	8.3
Traupel	3.2	5.9	14.1	22.7

Table 5: Comparison between the CFD results and the loss models.

blade design, comparable with the performance predicted at a preliminary design level. However, CFD results show that, due to the complexity of the fluid-dynamic phenomena involved (shock wakes and vortex interactions), there is indeed room to further improve the actual efficiency of the blade by resorting to advanced shape optimization methods. Finally the loss models used for the preliminary design of the turbine were assessed against CFD predictions. For the specific application here considered the Traupel's model outperforms the Craig & Cox model, which fails in reproducing secondary and tip phenomena. Hence, the use of the Traupel's model at a preliminary design level may lead to a more reliable design for such unconventional turbines.

NOMENCLATURE

NICFD	Not Ideal Compressible Fluid-Dynamics	
ROT	Radial-Outflow Turbine	
TBM	Turbine Blade Modeler	
β	blade and flow angles	(°)
γ	stagger angle	(°)
LE	leading-edge	
TE	leading-edge	
P	pressure	(bar)
T	temperature	(C°)
N	rotational speed	(rpm)
blh	blade height	(rpm)
c	blade chord	(m)
cl	camber-line length	(m)
o	throat width	(m)
tcl	tip-clearance	(m)
$\dot{m}$	mass flow	(kg/s)
M	flow Mach number	$(-)$
ζ_{is}	kinetic energy loss coefficient	$(\%)$
ew	eulerian work	(kJ/kg)
TD	thickness distribution	
SS	suction side	
PS	pressure side	
CPs	control points	
w	weight of the NURBS	

Subscript

is	isentropic
int	intersected
l	linear
th	thickness

REFERENCES

Angelino, G., Gaia, M., and Macchi, E. (1984). A review of Italian activity in the field of Organic Rankine Cycles. In *VDI Berichte - Proceedings of the International VDI Seminar*, volume 539, pages 465--482, Düsseldorf. VDI Verlag.

Casati, E., Vitale, S., Pini, M., Persico, G., and Colonna, P. (2014). Centrifugal Turbines for Mini-Organic Rankine Cycle Power Systems. *ASME Journal of Engineering for Gas Turbines and Power*, 136(122607):1--11.

Craig, H. and Cox, H. (1971). Performance estimation of axial flow turbines. *Proceedings Institution of Mechanical Engineers*, 185-32/71:407--424.

D'Amelio, L. (1935). *Impiego di vapori ad alto peso molecolare in piccole turbine e utilizzazione del calore solare per energia motrice*. Industria Napoletana Arti Grafiche.

Falck, D. and Collette, B. (2012). *FreeCAD [How-to]*. Packt Publishing.

Ghidoni, A., Pelizzari, E., Rebay, S., and Selmin, V. (2006). 3d anisotropic unstructured grid generation. *International journal for numerical methods in fluids*, 51(9□10):1097--1115.

Macchi, E. (1977). *Lecture series 100 on Closed-Cycle gas turbines*, chapter Design criteria for turbines operating with fluids having a low speed of sound. Von Karman Institute for Fluid Dynamics.

Macchi, E. (1985). Design limits: basic parameter selection and optimization methods in turbomachinery design. volume 97 Av 2, pages 805--828, Izmir, Turk. Martinus Nijhoff Publ., Dordrecht, The Netherlands.

Persico, G., Pini, M., Dossena, V., and Gaetani, P. (2013). Aerodynamic Design and Analysis of Centrifugal Turbine Cascades. In *ASME Turbo Expo 2013*, number GT2013-95770.

Persico, G., Pini, M., Dossena, V., and Gaetani, P. (2015). Aerodynamics of Centrifugal Turbine Cascades. *Journal of Engineering for*, 19.

Piegl, L. and Tiller, W. (1997). *The NURBS Book (2Nd Ed.)*. Springer-Verlag New York, Inc., New York, NY, USA.

Pini, M., Persico, G., Casati, E., and Dossena, V. (2013). Preliminary design of a centrifugal turbine for organic Rankine cycle applications. *Journal of Engineering for Gas Turbines and Power-Transactions of the ASME*, 135:042312--1--9.

Pini, M., Persico, G., Pasquale, D., and Rebay, S. (2014). Adjoint method for shape optimization in real-gas flow applications. *Journal of Engineering for Gas Turbines and Power*, 137(3):032604--032604.

Tabor, H. and Bronicki, L. (1964). Establishing criteria for fluids for small vapor turbines. In *SAE National Transportation, Powerplant, and Fuels and Lubricants Meeting*, number 640823.

Traupel, W. (1977). *Thermische Turbomaschinen*. Springer-Verlag, Berlin.

Verneau, A. (1987). *Lecture series 1987-07*, chapter Small high pressure ratio turbines. Supersonic turbines for organic Rankine cycles from 3 to 1300 kW. Von Karman Institute for Fluid Dynamics.

Vestraete, T. (2010). CADO: a Computer Aided Design and Optimization Tool for Turbomachinery Applications. 2nd International Conference on Engineering Optimization.

Vitale, S., Gori, G., Pini, M., Guardone, A., Palacios, F., Economon, T., Alonso, J., and Colonna, P. (2015). Extension of the SU2 Open Source CFD code to the simulation of turbulent flows of fluids modelled with complex thermophysical laws. In *AIAA 22th Computational Fluid-Dynamics Conference*, number CFD-16, 2148971, Dallas.

Zweifel, O. (1945). The spacing of turbo-machine blading especially with large angular deflection. *Brown Boveri Review*.

ACKNOWLEDGEMENT

Salvatore Vitale would like to acknowledge the FPP master student Roel de Koning, for his collaboration on the development of the TBM, and the support of the STW and Dana Spicer on the CC-PowerTrain project.